ISSN: 1692-7257 - Volume 2 – Issue 48 - 2026

ORIGINAL

RCTA
Revista Colombiana de Tecnologías de Avanzada
UNIPAMPLONA

Design, implementation, and functional validation of a short-range LoRa-based underwater monitoring architecture

Diseño, implementación y validación funcional de una arquitectura de monitoreo subacuático de corto alcance basada en LoRa

Diego Arbey Montezuma Rosero[1]
Fabián Geovanny Cuzme Rodríguez[1]
Jaime Roberto Michilena Calderón[1]
Luis Edilberto Suárez Zambrano[1]

[1] **Universidad Técnica del Norte, Facultad de Ingeniería en Ciencias Aplicadas, Av. 17 de Julio 5-21 y General José María Córdova, Ibarra 100105, Ecuador.**

Received: 26 May 2026. Revised: 26 June 2026. Accepted: 31 July 2026. Published: 04 August 2026.
Corresponding Author: Fabián Geovanny Cuzme Rodríguez

How to cite: D. A. Montezuma Rosero, F. G. Cuzme Rodríguez, J. R. Michilena Calderón, and L. E. Suárez Zambrano, "Diseño, implementación y validación funcional de una arquitectura de monitoreo subacuático de corto alcance basada en LoRa", *Revista Colombiana de Tecnologías de Avanzada (RCTA)*, vol. 2, no. 48, ago. 2026, art. no. 4509, doi: 10.24054/rcta.v2i48.4509

This work is licensed under a Creative Commons Attribution-NonCommercial 4.0 International License.

Abstract:

Environmental monitoring in aquatic ecosystems requires communication systems capable of operating under the particular conditions of underwater environments. This work presents the design, implementation, and functional validation of a short-range underwater monitoring system based on LoRa technology for freshwater environments. The developed architecture integrates a submerged sensor node for environmental data acquisition, a communication buoy located at the water surface, and a web platform for real-time data visualization. Communication between the sensor node and the buoy is performed through a LoRa link operating in the 915 MHz ISM band under an underwater-to-overwater (UW2OW) configuration, while data transmission to the cloud is carried out through a 2.4 GHz Wi-Fi connection. Functional validation was conducted in a controlled environment consisting of a swimming pool and in natural freshwater environments represented by two lagoons, considering different node depths and horizontal separation distances. The maximum distance with detectable reception depended on the node depth and the test environment, ranging from 1.2 to 13 m. However, packet loss increased considerably near these limits; therefore, more conservative operational reference distances were established. Operational limitations related to node depth, packet loss, transmission delay, and effective receiver sensitivity were also identified. The results demonstrate the functional feasibility of the proposed architecture for low-dynamic environmental monitoring applications and provide an experimental basis for future improvements to the communication system and deployment mechanisms in aquatic environments.

Keywords: underwater communication, LoRa, environmental monitoring, wireless sensor networks, telemetry.

Resumen:

El monitoreo ambiental en ecosistemas acuáticos requiere sistemas de comunicación capaces de operar bajo las condiciones particulares del medio subacuático. En este trabajo se presenta el diseño, implementación y validación funcional de un sistema de monitoreo subacuático de corto alcance basado en la tecnología LoRa para ambientes de agua dulce. La arquitectura desarrollada integra un nodo sensor sumergido para la adquisición de variables ambientales, una boya de comunicaciones ubicada en superficie y una plataforma web para la visualización de la información en tiempo real. La comunicación entre el nodo sensor y la boya se realiza mediante un enlace LoRa en la banda ISM de 915 MHz bajo una configuración underwater-to-overwater (UW2OW), mientras que la transmisión hacia la nube se efectúa mediante Wi-Fi a 2.4 GHz. La validación funcional se realizó en un entorno controlado (piscina) y en ambientes naturales (lagunas de agua dulce), evaluando el comportamiento operativo del sistema bajo diferentes profundidades y distancias de separación entre el nodo y la boya. Los resultados muestran que la distancia máxima con recepción detectable dependió de la profundidad y del escenario evaluado, con valores comprendidos entre 1.2 y 13 m. No obstante, la pérdida de paquetes aumentó considerablemente al aproximarse a estos límites, por lo que se establecieron distancias operativas de referencia más conservadoras. Asimismo, se identifican limitaciones operativas asociadas con la profundidad, la pérdida de paquetes, el retardo de transmisión y la sensibilidad efectiva del sistema, aspectos que deben considerarse durante el despliegue de este tipo de soluciones. Los resultados obtenidos demuestran la factibilidad funcional de la arquitectura propuesta para aplicaciones de monitoreo ambiental de baja dinámica y proporcionan una base experimental para futuras optimizaciones del sistema de comunicación y de los mecanismos de despliegue en ambientes acuáticos.
Palabras clave: comunicación subacuática, LoRa, monitoreo ambiental, redes de sensores inalámbricos, telemetría.

INTRODUCTION

Underwater communications have developed significantly in recent years [1]. Nevertheless, their implementation remains a challenge because of the propagation conditions of the medium, which impose limitations on bandwidth, propagation speed, data transfer rate, device power supply, and the complexity of infrastructure deployment [2]. To address these restrictions, underwater communications have developed mainly along acoustic, optical, and electromagnetic lines. Acoustic communication is one of the most widely used approaches in underwater environments, because sound waves can propagate over long distances in water. However, its operation may be limited by ambient noise, latency, energy consumption, and variations in the medium [3]. Optical communications, in turn, allow high transfer rates but require favorable alignment and visibility conditions. Absorption, scattering, and water turbidity considerably reduce their range [4].

The third approach is electromagnetic communication via radiofrequency, on which this work focuses. Electromagnetic waves offer advantages associated with their low latency and the possibility of using compact communication devices; however, they undergo high attenuation when propagating in aquatic media, especially as the operating frequency, water conductivity, and device depth increase [5]. Consequently, their application is mainly oriented toward short-range underwater links. LoRa technology uses chirp spread spectrum modulation, called Chirp Spread Spectrum (CSS) [6], and was developed for long-range, low-power wireless communications [7]. Its high reception sensitivity and the robustness of its modulation make it a candidate for short-range underwater links. However, its performance in these environments depends on the characteristics of the aquatic medium, the depth, the operating frequency, the radio configuration, and the physical implementation of the antennas.

This work proposes the design and implementation of a short-range underwater monitoring system based on LoRa technology for freshwater environments. The architecture integrates a submerged sensor node that acquires environmental variables, a communication buoy at the surface that receives and retransmits the information, and a web platform that stores and visualizes the data. The study is oriented toward the functional validation of this complete architecture in controlled and natural scenarios, considering the operational limitations observed during its deployment[8].

Within the framework of this research, previous works were identified in which experimental tests were carried out with communication nodes located in aquatic environments; one of them proposes the use of the 433 MHz frequency through the use of TWS-433 RF transmission and reception modules, where 2 nodes located on the water surface (OW2OW) are used and a maximum signal propagation distance of up to 9 m is achieved[5]. Another of the studies uses higher frequencies to evaluate data transmission in an underwater environment, with a transmitter and receiver depth of 0.15 m, which allows data transfer of up to 0.16 m in a 2.4 GHz frequency band[3]. Not leaving aside technologies such as Bluetooth that operate in the same frequency band, it has been used in a study generated through a test environment in a fish tank, for both freshwater and saltwater, with the use of 2 nodes separated by a few centimeters (UW2OW), reaching a propagation distance of up to 0.19 m[4].

Regarding the use of LoRa technology, there is a study in Dishui Lake in Shanghai that uses the 433 MHz frequency with similar Spreading Factor and bandwidth parameters, evaluating 3 modes: submerged transmitter and submerged receiver (UW2UW), submerged transmitter and receiver on the water surface (UW2OW), and transmitter on the surface and submerged receiver (OW2UW). The links with one submerged node and one on the surface performed best[9]. Studies have also been carried out through the design of an antenna for LoRa communication at 868 MHz frequencies, where a distance of 0.6 m was reached when the nodes are submerged in water[10].

In a later investigation, Pozzebon et al. evaluated LoRaWAN transmissions from water to the surface through laboratory and field tests in saltwater. The results showed that reception can be maintained when the transmitter is at a shallow depth, although reliability decreases considerably when approaching the receiver's sensitivity limits. This study confirms the importance of differentiating between detectable reception and reliable operation in aquatic applications[11].

Although previous works have demonstrated the possibility of using radiofrequency and LoRa technology for short-range underwater communications, most research has focused on the analysis of physical link behavior or on the isolated evaluation of communication modules. In contrast, studies presenting an integrated architecture for environmental monitoring that combines a submerged sensor node, a LoRa–Wi-Fi communication buoy and a remote supervision platform validated through experimental tests in real freshwater scenarios are scarce. This gap motivates the development of the system presented in this work.

In this context, the main contribution of this research is the design, implementation and functional validation of a short-range underwater monitoring architecture based on LoRa. The specific contributions are: i) the implementation of a submersible sensor node for the acquisition of environmental variables; ii) the development of a buoy that integrates LoRa and Wi-Fi communications for relaying data to the cloud; iii) the integration of a web platform for information storage and visualization; and iv) the functional validation of the system in controlled and natural scenarios, identifying operational limitations associated

with depth, packet loss, delay and the effective sensitivity of the prototype. The rest of the article is organized as follows. Section 2 describes the proposed architecture, the materials used and the experimental methodology employed for the design, implementation and validation of the system, as well as the simulation model used as a reference. Section 3 presents the experimental results obtained in the different evaluation scenarios. Section 4 discusses the results and compares them with related research, analyzing the main limitations and scope of the proposal. Finally, Section 5 presents the conclusions and future lines of work.

METHODOLOGY

Design

The system was implemented using two Heltec Wi-Fi LoRa 32 V3 boards, which integrate an ESP32-S3 microcontroller and LoRa, Wi-Fi and Bluetooth communications. One board was used in the sensor node and the second in the communication buoy. The sensor node acquires the pH and turbidity variables and transmits the information via LoRa at 915 MHz to the buoy located at the surface. Subsequently, the buoy relays the data via Wi-Fi to Firebase for storage and visualization through a web platform.

The architecture is composed of three elements: i) a sensor node submerged at the depth defined for each trial; ii) a communication buoy that receives the packets under a UW2OW configuration; and iii) a web platform for remote storage and visualization. LoRa communication is carried out through a point-to-point link between the two Heltec boards, while the Wi-Fi connection is used exclusively between the buoy and the cloud platform.

The Heltec Wi-Fi LoRa 32 V3 board was selected because it integrates the SX1262 transceiver and the ESP32-S3 microcontroller in a single device, supports a transmission power of up to 21 dBm and can be programmed through the Arduino IDE environment. Its main characteristics are summarized in Table 1.

Table 1: Technical data of the Heltec Wi-Fi LoRa 32 V3 board

	Specification
Microcontroller	ESP32
LoRa chip	SX1262
Power consumption	<10 µA
Operating frequency	863–928 MHz / 470–510 MHz
Maximum power	21 ± 1 dBm
Maximum sensitivity	−137 dBm
Integrated technologies	Bluetooth, Wi-Fi, LoRa
Operating temperature	−20 °C to 70 °C
Operating voltage	3.7 V

Source: Heltec platform [12] and Semtech [20]

The parameters used to configure LoRa signal transmission were chosen on the basis of signal range and robustness in hostile environments, since their configuration directly affects propagation. Aspects such as transmission speed and data rate are tied to settings such as the Spreading Factor, whose highest configuration, SF12, makes the signal more robust against interference and increases its range, improving sensitivity in data reception. Likewise, the Coding Rate allows more redundancy bits to be used for error correction, which is ideal for environments with high loss rates. The use of low bandwidth values such as 125 kHz also allows a greater signal range at the expense of the amount of data.

The communication parameters used are: frequency, transmission power, bandwidth, signal spreading factor, coding rate and preamble length. All of these are set in a configuration aimed at greater signal range and better signal robustness; Table 2 presents the respective configurations.

Architecture

Given the parameters with which the Heltec Wi-Fi 32 V3 board has been configured, the next step is to propose a system that allows monitoring a submerged environment through the implementation of the 2 aforementioned nodes, using LoRa for communication in the submerged environment and Wi-Fi for transmitting data to the Firebase database, so that these are stored and displayed on a web platform in real time.

Table 2: Parameters configured for transmission

	Configuration
Frequency	915 MHz
Power	21 dBm
Bandwidth	125 kHz
Spreading Factor	SF12
Coding Rate	4/8
Preamble length	12 symbols

Source: own elaboration

The process begins with the sensor node, which is submerged in the water at a depth x and is equipped with sensors that capture environmental variables such as the pH and turbidity of the water. This node processes the information in real time and transmits it using the 915 MHz band to a communication buoy at the water surface, which contains a reception antenna configured to the same frequency. Because the transmission of electromagnetic signals in aquatic media presents high attenuation, the buoy acts as a nearby repeater that receives the LoRa signal coming from the submerged node and retransmits it through a Wi-Fi link (2.4 GHz). Once the communication buoy receives the data from the sensor node, it uses this Wi-Fi antenna integrated into the Heltec LoRa Wi-Fi 32 V3 module to connect directly to the internet. Through this connection, the buoy sends the data to Firebase in real time.

A user monitoring this link can view these data through a web interface, which connects to the Firebase database to retrieve the information and display it in graphs that allow it to be interpreted. In this way, continuous monitoring of the water conditions is achieved. Fig. 1 shows the architecture of the system.

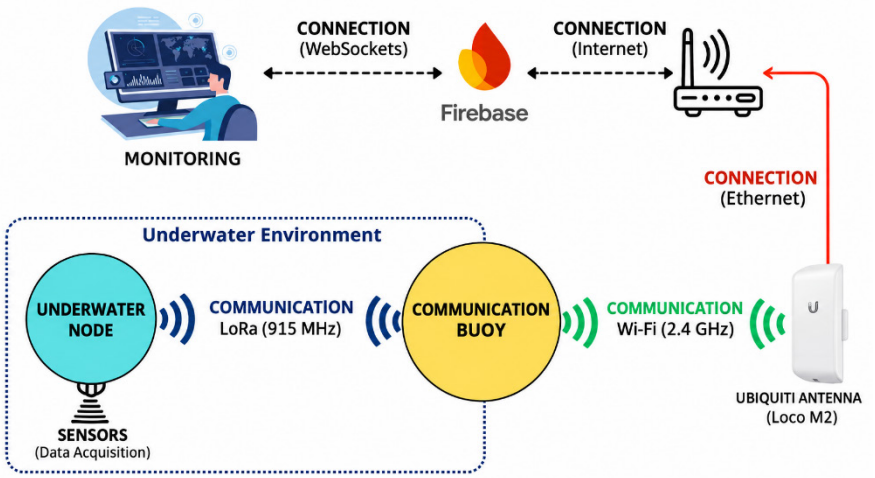

Fig. 1. *Architecture of the system.*
Source: own elaboration.

System functionality

The complete process of the system's operation is presented in Fig. 2, which shows the interaction between the different sections of the system, in order to fulfill the objective of monitoring environmental variables through the use of LoRa communication.

The system executes an initial stage in both the sensor node and the communication buoy. Here, the communication parameters are configured, the hardware is turned on and the processes necessary for the system startup are executed. When the system has started on both devices, the sensor node reads the data coming from the sensors in contact with the water. These data are stored in the flash memory of the Heltec Wi-Fi 32 V3 board using variables, then a structured data packet is generated containing all the information in a text string.

Before transmitting this data string, if the system starts for the first time, it will perform a check to verify whether the buoy is available to receive packets. If the receiver responds positively, the transmission process begins (the sensor node verifies that the buoy is online every so often, in order not to send packets unnecessarily). Whenever a packet is transmitted, a function is executed that releases the LoRa communication module for the next transmission and an LED turns on indicating that the packet has been sent.

As for the communication buoy, after the system starts, a connection to the Wi-Fi network is established. Once the connection is established, a request is sent to an NTP server to synchronize the current time. Subsequently, the buoy connects to the database (Firebase) and the system waits for packets to arrive through the LoRa module. When a packet reaches the LoRa communication module, the indicator LED turns on and the packet is stored as a text string in the Flash memory. Then, it extracts the values individually and stores them in separate variables, while displaying them on the OLED screen of the Heltec Wi-Fi LoRa 32 V3 device.

Finally, the data are sent to Firebase both for storage in the data history and for real-time updating. Once this process is complete, the system enters standby mode to receive new data. As for the user interface, since it is based on a web page, a request is made to Firebase to obtain the updated values. These are interpreted visually through historical graphs and can also be viewed in real time as they arrive from the system (see Fig. 2).

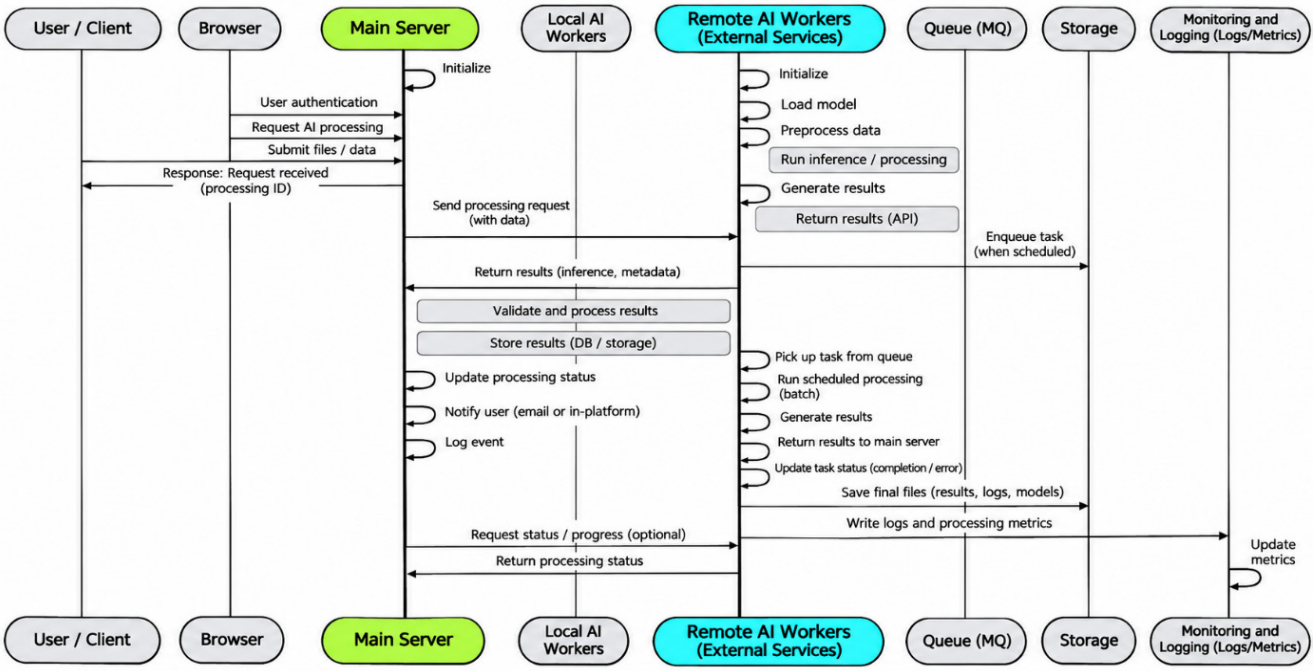

Fig. 2. *System sequence diagram.*
Source: own elaboration.

Sensor node design

The sensor node is the most exposed component of the system, since it must operate submerged at a given depth; therefore, its electronic elements require hermetic protection. As shown in Fig. 3, the node integrates pH and turbidity sensors, signal conditioning modules, a Heltec Wi-Fi LoRa 32 V3 board and a LoRa antenna connected through the U.FL interface. The board receives, processes and transmits the data acquired by the sensors through the ESP32 pins. The system is powered by a 3.7 V battery and uses a 3.7 to 5 V converter to supply the voltage required by the sensors.

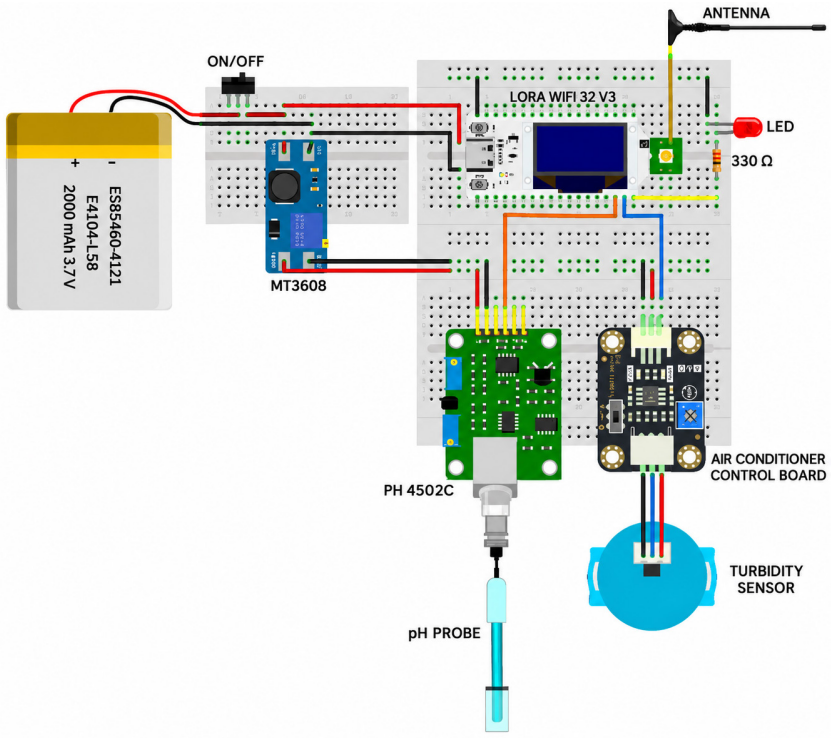

Fig. 3. *Connection diagram of electronic modules (Sensor Node).*
Source: own elaboration.

The electronic components of the sensor node are housed in a 3D-designed hermetic enclosure to protect them against leaks during underwater tests. The spherical structure is divided into an upper and a lower section, joined by an intermediate thread that allows access to the interior and facilitates assembly and maintenance of the system.

The upper section incorporates a compartment for the lithium polymer battery, a base for fixing the PCB, an external handle for holding and recovering the node by means of ropes, and protected openings for the LED indicator and the LoRa antenna. These elements were designed to maintain the watertightness of the assembly and to protect both the electronic components and the connections exposed to the aquatic environment; these features can be seen in Fig. 4.

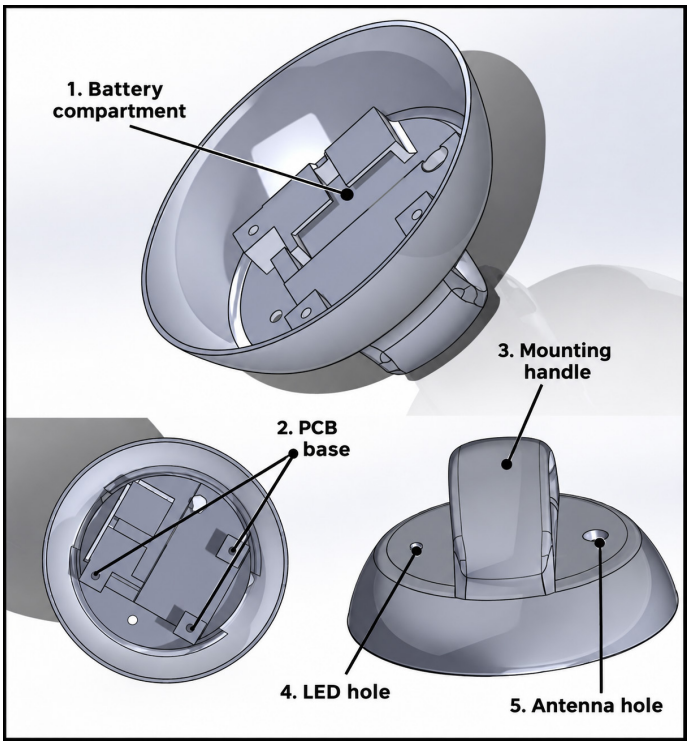

Fig. 4. *Upper cover design (Sensor Node).*
Source: own elaboration.

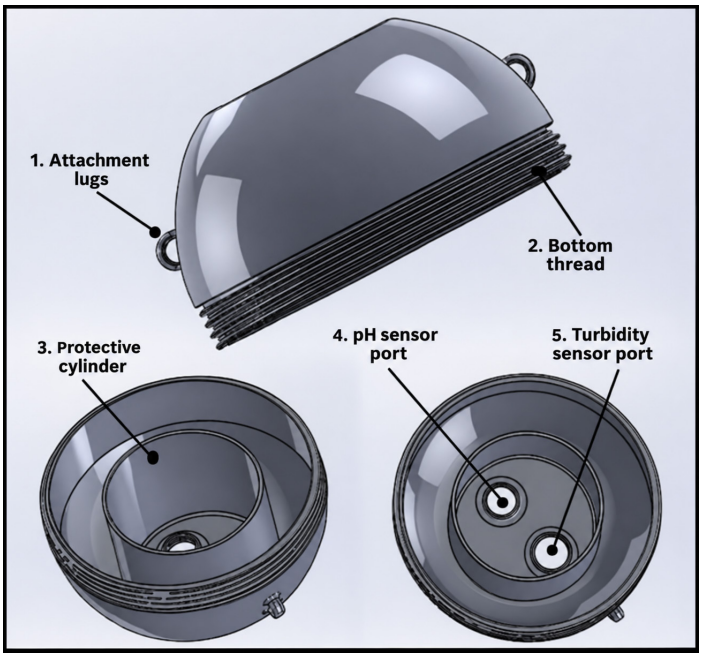

Fig. 5. *Lower cover design (Sensor Node).*
Source: own elaboration.

The lower cover of the sphere, shown in Fig. 5, is intended for the integration of the sensors and for controlling the immersion of the node. This section incorporates rings and cavities for adding weight, a thread for joining it to the upper cover and a central protective cylinder. In addition, it includes threaded holes for the safe installation of the pH and turbidity sensors, maintaining the mechanical protection and sealing of the assembly.

Communication Buoy Design

The electronic schematic of the communication buoy centers on the Heltec Wi-Fi LoRa 32 V3 module. In this case, the connection is simpler; the board is powered by a 3.7 V battery. The integrated LoRa board receives the data through the LoRa antenna operating at 915 MHz and retransmits them to Firebase through its Wi-Fi module integrated in the ESP32 microcontroller (see Fig. 6).

Web platform design

The data visualization platform was set up using Firebase, since it facilitates real-time synchronization between the devices that connect to the platform; it does so by storing the data in JSON format, as it is a NoSQL (non-structured) database[13]. The database used contains 8 branches, each with information inside stored variables; here 2 types of data are defined (history and realtime). Fig. 7 shows the general structure.

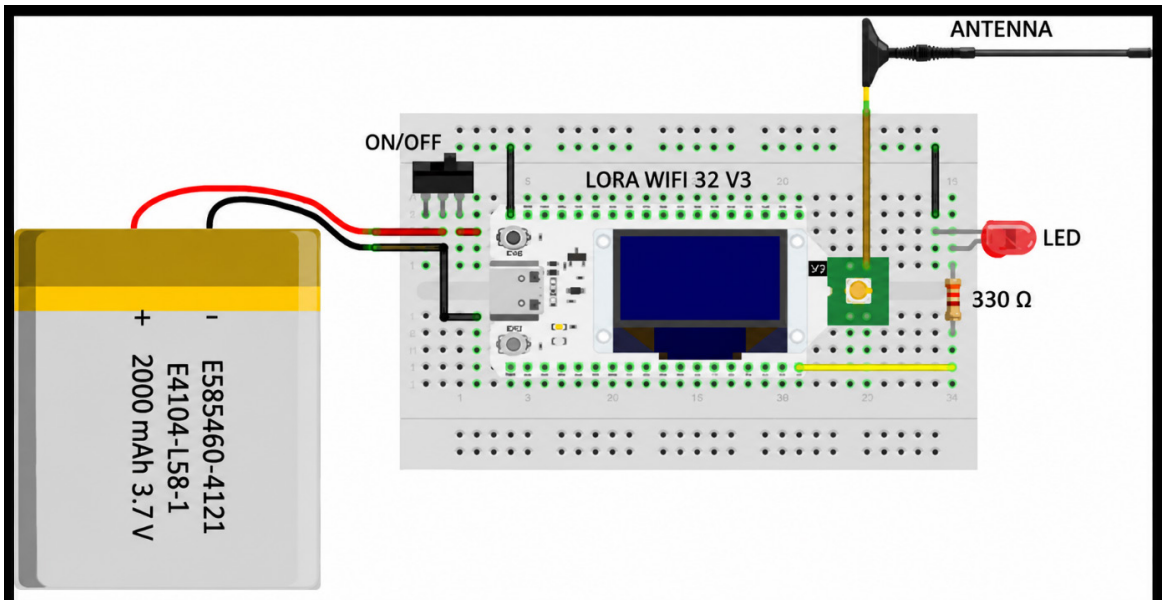

Fig. 6. *Connection diagram of electronic modules (communication buoy).*
Source: own elaboration.

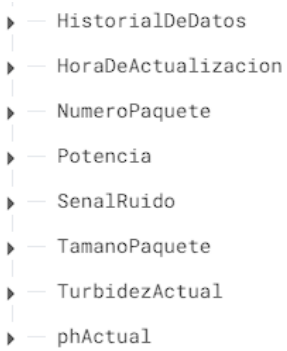

Fig. 7. *Data tree in Firebase.*
Source: own elaboration.

A branch named “HistorialDeDatos” is established, where the information arriving from the communication buoy is stored as a historical record; these are stored based on a “Timestamp” that contains a structure with all the collected data, which subsequently allows historical graphs of them to be generated (see Fig. 8-a). On the other hand, the data updated in real time are stored as variables; these change automatically when the information is uploaded to the platform from the buoy (see Fig. 8-b).

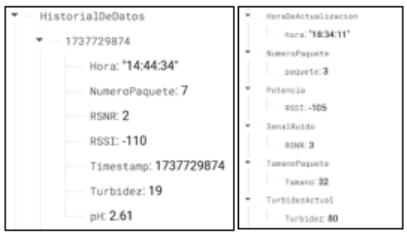

Fig. 8. *Data history (a) and real-time data (b) captured from Firebase.*
Source: own elaboration.

The user interface was designed around the development of a web page using programming languages such as HTML, CSS and JavaScript; this platform takes the 2 types of data stored in Firebase (history and realtime). Fig. 9 shows the data as cards generated on the Web, where the information is loaded in real time as it is updated in Firebase.

Another way of presenting the information on the Web is through historical graphs, which allow visualizing how the data evolve over time; for this purpose, the tree generated through the "HistorialDeDatos" branch in Firebase is used, as shown in Fig. 10.



Fig. 9. *Real-time data presentation cards.*
Source: own elaboration.

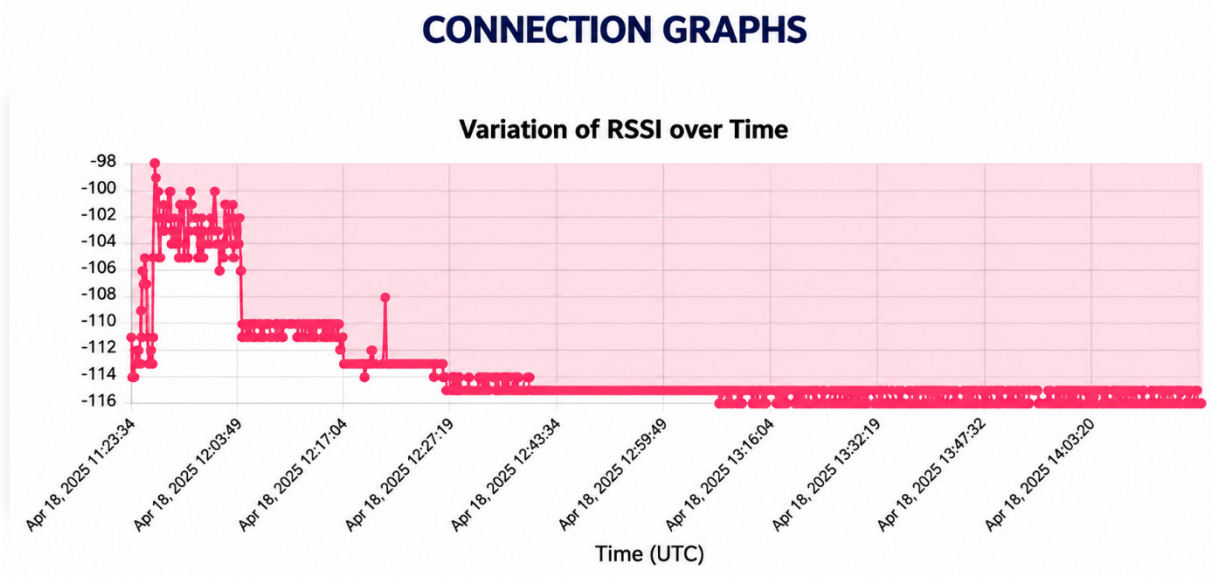

Fig. 10. *Data history presentation graph.*
Source: own elaboration.

Implementation

Sensor node

The construction of the sensor node, which houses the electronic elements and the sensors, was carried out using the 3D-printed design specified above. It has a hermetic structure to protect the components in the aquatic environment. The design includes four openings: two for the output of the sensors in direct contact with the water, one for the LoRa antenna and another for an LED operating indicator. Its already implemented structure, both internal and external, is shown in Fig. 11.



Fig. 11. *Sensor node, internal part (a) and external part (b).*
Source: own elaboration.

Communication buoy

The construction of the communication buoy, which houses the electronic elements, is carried out on a floating material, in this case, polystyrene. The LoRa antenna remains in contact with the water surface; in addition, the module's 2.4 GHz antenna is used to establish the Wi-Fi connection to the Internet. The design of the buoy is shown in Fig. 12. It should be noted that a hermetic outdoor electrical box has been used that complies with an IP65 standard, for protection against dust and projected water[14].

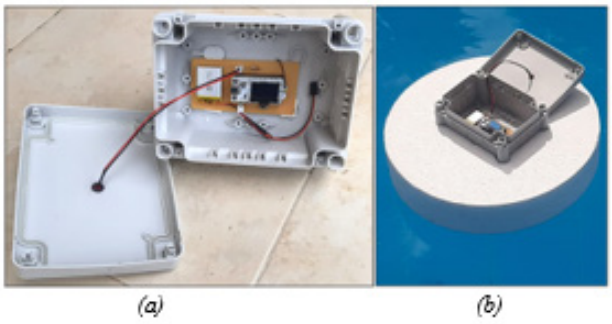

Fig. 12. *Communication buoy, internal part (a) and external part (b).*
Source: own elaboration.

Experimental protocol

The tests were organized considering the evaluation scenario, the depth of the sensor node and the horizontal distance between the submerged node and the communication buoy. For each combination of scenario, depth and distance, two independent tests were performed; in each one, 50 packets were transmitted, with an interval of 10 s and a payload of 60 bytes. During all tests, the LoRa configuration was kept constant: frequency of 915 MHz, transmission power of 21 dBm, bandwidth of 125 kHz, SF12, CR 4/8 and preamble of 12 symbols.

For each correctly received packet, the packet identifier, RSSI, SNR, payload size and the timestamps used to calculate the delay were stored. The reported delay corresponds to the data transfer between node and buoy; it was calculated as the difference between the time at which the packet is timestamped when transmitted from the LoRa module of the sensor node and the time at which the packet is timestamped when captured by the buoy. Before starting each test, the clocks used by the sensor node and the buoy were synchronized using the NTP server as presented in Fig. 2. Packet loss was obtained using the equation presented in(1).

$$PER = \frac{N_{tx} - N_{rx}}{N_{tx}} \quad (1)$$

Where N_{tx} corresponds to the number of transmitted packets and N_{rx} to the number of correctly received packets. For RSSI, SNR and delay, the mean and standard deviation of the received packets were calculated for each experimental condition. To interpret the results, two concepts were distinguished.

The reference operating distance was defined as the greatest separation at which the packet loss percentage was equal to or less than 50 %. This threshold was adopted solely as an internal criterion to compare the operating conditions of the prototype and does not imply fully reliable communication. The maximum distance with detectable reception corresponds, in contrast, to the greatest separation at which at least one packet was received, even if the link presented high losses.

MATLAB simulation

The simulation presented in this research is referential in nature and was used to estimate the expected propagation trend of the electromagnetic link under ideal conditions. Due to the complexity of the underwater medium, the model does not fully consider phenomena such as antenna orientation, device encapsulation, the water–air interface or local variations in the physicochemical properties of the water. Consequently, the simulated results are used only as a reference to contrast the behavior observed experimentally.

One of the parameters used is the conductivity of the medium, which is set between 300 and 1500 µS/cm in freshwater environments [15]. For the simulation, a conductivity of 560 µS/cm was used, taking as reference the value reported for the Yahuarcocha lagoon [16]. A relative permittivity of water of 80 [17], a vacuum permittivity of 8.85×10^{-12} F/m and a bandwidth of 125 kHz were also used (see Fig.13). Because these parameters do not represent all the spatial and temporal variability of natural scenarios, the model results are used only as a theoretical reference and not as an exact prediction of the system range.

```
% Parámetros físicos
f = 915e6; % Frecuencia en Hz (915 MHz)
d = [0.1, 1:0.5:15]; %distancia
c = 3e8; % Velocidad de la luz en m/s
Pt_dBm = 21; % Potencia de transmisión en dBm
Pt = 10^((Pt_dBm - 30)/10); % Conv. dBm a Watts
epsilon_r = 80; % Permitividad relativa
sigma = 560e-6; % Conductividad para agua dulce
epsilon_0 = 8.85e-12; % Permitividad del vacío
omega = 2 * pi * f; % Frecuencia angular
```

Fig. 13. *Data variables for simulation.*
Source: own elaboration.

Because water absorbs electromagnetic waves due to the electrical conductivity (σ) of the medium, an equation is established to model this absorption, using an attenuation coefficient (α) measured in nepers per meter (Np/m). The equation in(2)allows this attenuation coefficient to be calculated in highly lossy media[18]. The values considered here are the angular frequency ($2\pi f$), the permittivity of the medium (ε), the electrical conductivity of the medium (σ) and the operating frequency (f).

$$\alpha = \frac{\omega}{c}\sqrt{\frac{\varepsilon_r}{2}\left(\sqrt{1+\left(\frac{\sigma}{\varepsilon_0\omega}\right)^2}-1\right)} \quad (2)$$

Another important parameter taken into account in the simulated environment is the calculation of the SNR at different distances, for which the equation in(3)is used; it gives the general formula for the thermal noise power in a communications system[18]. The equation uses values such as the system noise figure (NF), the Boltzmann constant (k), the equivalent noise temperature (T) and the bandwidth (B).

$$N_0 = (NF)kTB \quad (3)$$

Test environments

The functional validation was carried out in three aquatic scenarios. The first scenario was a swimming pool 12 m long and 6.5 m wide. For the comparison presented in Table 3, the antenna of the sensor node was placed at a depth of 0.8 m relative to the antenna of the buoy, while the horizontal distance was progressively increased from 1 m until packet reception was lost. The horizontal distance was measured on the water surface between the vertical projection of the node's location and the position of the buoy, as shown in Fig. 14.

The second scenario was the Yahuarcocha lagoon, located in Ibarra, Imbabura province. This body of water was selected for its turbidity conditions and for the reference conductivity value reported in[16]. The tests kept the UW2OW configuration and the horizontal measurement procedure used in the swimming pool, evaluating depths of 0.25, 0.5 and 0.8 m, as shown in Fig. 15.

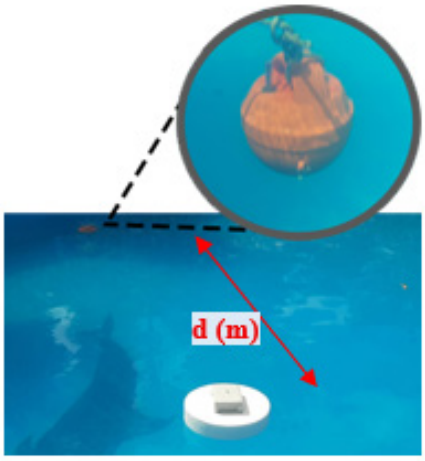

Fig. 14. *Test environment in the swimming pool.*
Source: own elaboration.



Fig. 15. *Test environment in the Yahuarcocha lagoon.*
Source: own elaboration.

The third scenario was the San Pablo lagoon, located in Imbabura province, near the city of Otavalo, Ecuador. This scenario was selected because its visual turbidity conditions differed from those observed in Yahuarcocha. The tests were carried out with the same UW2OW configuration, the same depths and the same horizontal measurement procedure used in the previous scenarios, as shown in Fig. 16.

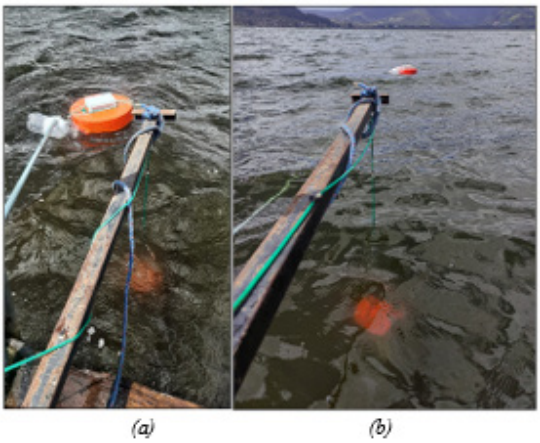

Fig. 16. Test environment at Laguna de San Pablo. Buoy suspended in the water (a) and submerged sensor node (b)
Source: own elaboration.

RESULTS

The results are presented in three sections. First, the results of the reference model implemented in MATLAB are shown. Then, the measurements obtained during the functional validation of the system in the swimming pool and in the Yahuarcocha and San Pablo lagoons are presented. Finally, the storage and visualization of the environmental data through Firebase and the web platform are verified. The simulation and the experimental measurements are analyzed as complementary elements, without assuming that the theoretical model exactly reproduces the conditions of the natural scenarios.

Simulation results

The estimated values of received power and signal-to-noise ratio as a function of distance are presented in Fig. 17. For the SF12 configuration and a BW of 125 kHz, a nominal sensitivity of −137 dBm was used as a reference[20]. This value corresponds to the theoretical performance of the transceiver under controlled conditions and does not directly represent the effective sensitivity of the complete prototype in the experimental scenarios.

In this analysis, the distances evaluated range from 0.1 m, which corresponds to the depth of the antenna located in the communication buoy, to 15 m of separation between both nodes. Under the parameters assumed in the simulation, the estimated power crosses the nominal threshold at approximately 12.5 m (see Fig. 17-a). Therefore, this distance represents only a theoretical reference of the model. It should not be interpreted as the guaranteed practical range of the system, because the simulation does not fully incorporate the losses caused by the antenna, the enclosure, the water–air interface, the orientation, the environmental noise and the variability of the aquatic medium.

The simulated signal-to-noise ratio decreases with distance until it approaches −20 dB (see Fig. 17-b). This value is used as a reference to interpret the degradation of the link; however, practical reception depends on the joint action of RSSI, SNR, packet loss and the physical conditions of the system. Consequently, the simulation allows a trend to be observed, but the operating distance must be determined from the functional tests.

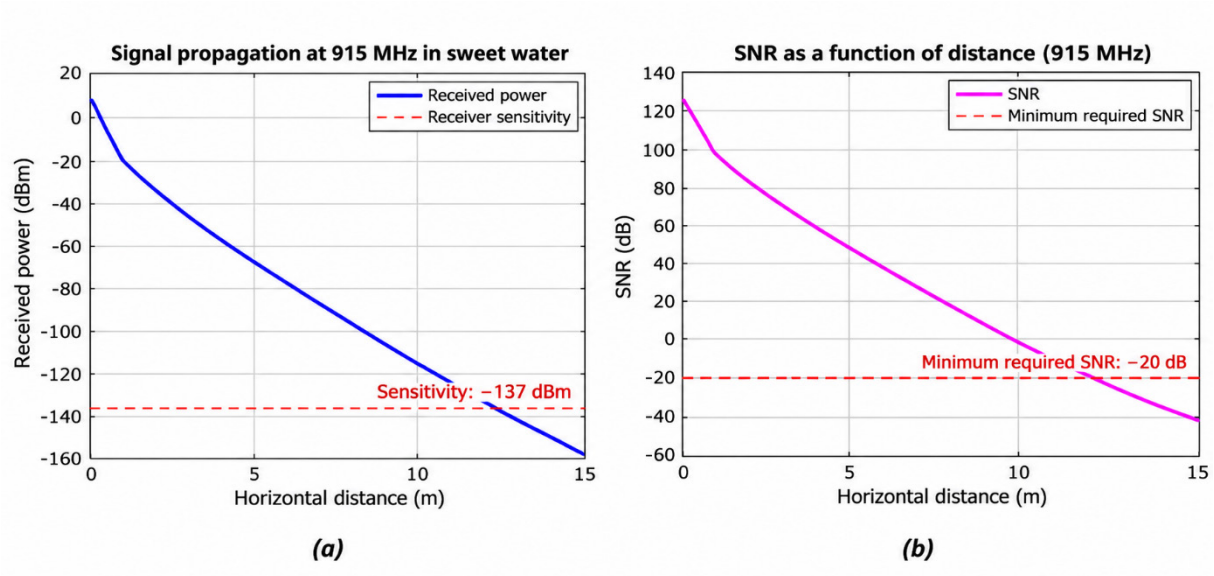

Fig. 17. *Signal propagation plots at 915 MHz. Received signal power plot (a) and signal-to-noise ratio plot (b). Source: own elaboration.*

Test environment results

For the functional validation of the system, a fixed configuration of SF12, BW of 125 kHz and CR 4/8 was maintained. SF12 was selected for its high nominal sensitivity [20] and for its orientation toward robust low-data-rate links. This article does not perform an experimental comparison between different Spreading Factor values, because the objective is to verify the operation of the complete architecture under a constant configuration. Distances were measured horizontally on the water surface from the projection of the submerged node's location to the position of the buoy.

Table 3 summarizes the metrics obtained during the functional validation of the system at a depth of 0.8 m in the swimming pool and in the San Pablo and Yahuarcocha lagoons. For each scenario, the maximum distance with detectable reception, the reference operating distance, the number of packets transmitted and received, the packet loss, RSSI, SNR and delay are presented.

Table 3: Connection tests at a depth of 0.8 m in the 3 environments

	Swimming pool	S. P. lagoon	YAH. lagoon
Maximum distance measured with detectable reception	11.4 m	4.5 m	1.2 m
Reference operating distance	10 m	3.5 m	0.8 m
Packets transmitted at maximum distance N_{tx}	100	100	100
Packets received at maximum distance N_{rx}	16	16	3
Packet loss at maximum distance	84%	84%	97%
Packet loss at reference operating distance	30%	50%	40%
Mean RSSI ± standard deviation at maximum distance	−116 ± 0.5 dBm	−116 ± 0.45 dBm	−116 ± 0.38 dBm
Mean SNR ± standard deviation at maximum distance	−20 ± 1.33 dB	−18 ± 2.27 dB	−18 ± 0.6 dB
Mean delay ± standard deviation at maximum distance	5942 ± 532 ms	6237 ± 598 ms	5650 ± 504 ms

Source: own elaboration

At a depth of 0.8 m, the greatest distance with detectable reception was 11.4 m in the swimming pool, 4.5 m in San Pablo and 1.2 m in Yahuarcocha. However, in all three scenarios packet loss increased considerably near these distances. For this reason, the maximum values represent marginal reception conditions and not reliable operating distances. The reference operating distances were shorter and were established according to the criterion defined in the methodology

Table 4 presents the metrics recorded at a depth of 0.5 m in the San Pablo and Yahuarcocha lagoons. The results are interpreted by distinguishing the marginal reception observed at the maximum distance from the system operation at the reference distance.

Table 4: Connection tests at a depth of 0.5 m in the San Pablo and Yahuarcocha lagoons

	L. SP	L. YAH
Maximum distance measured with detectable reception	7 m	4 m
Reference operating distance	5.5 m	3.5 m
Packets transmitted at maximum distance N_{tx}	100	100
Packets received at maximum distance N_{rx}	36	15
Packet loss at maximum distance	64%	85%
Packet loss at reference operating distance	42%	46%
Mean RSSI ± standard deviation at maximum distance	−116 ± 0.52 dBm	−116 ± 0.58 dBm
Mean SNR ± standard deviation at maximum distance	−17 ± 1.68 dB	−22 ± 2.65 dB
Mean delay ± standard deviation at maximum distance	6310 ± 505 ms	5398 ± 493 ms

Source: own elaboration

At a depth of 0.5 m, detectable reception was obtained up to 7 m in San Pablo and 4 m in Yahuarcocha. SNR values close to or below −20 dB were associated with a marginal link condition and with high packet loss percentages. Consequently, the occasional reception of packets was not interpreted as continuous or stable communication.

Table 5 summarizes the metrics obtained at a depth of 0.25 m in the San Pablo and Yahuarcocha lagoons. This depth presented the greatest distances with detectable reception among the natural scenarios; however, link reliability decreased as these distances were approached.

At a depth of 0.25 m, the greatest distances with detectable reception were recorded in the natural scenarios: 13 m in San Pablo and 8.5 m in Yahuarcocha. However, the losses of 73% and 98%, respectively, show that these distances correspond to the reception limit of the system. The referential operating distances were reduced to 12 m and 7.5 m under the stability criterion defined for the application.

Under the evaluated conditions, the reduction in depth was accompanied by an increase in the distance with detectable reception. Nevertheless, the differences between the scenarios cannot be attributed exclusively to turbidity, since conductivity, antenna orientation, water movement, encapsulation and ambient noise may also be involved. The mean delays were between approximately 5 and 6.4 s, so their effect is analyzed in Section 4.

Table 5: Connection tests at a depth of 0.25 m in the San Pablo and Yahuarcocha lagoons

	L. SP	L. YAH
Maximum distance measured with detectable reception	13 m	8.5 m
Reference operating distance	12 m	7.5 m
Packets transmitted at maximum distance N_{tx}	100	100
Packets received at maximum distance N_{rx}	27	2
Packet loss at maximum distance	73%	98%
Packet loss at reference operating distance	47%	36%
Mean RSSI ± standard deviation at maximum distance	−116 ± 0.4 dBm	−116 ± 0.5 dBm
Mean SNR ± standard deviation at maximum distance	−18 ± 2.5 dB	−23 ± 1.5 dB
Mean delay ± standard deviation at maximum distance	6403 ± 792 ms	5592 ± 485 ms

Source: own elaboration

The means and standard deviations were calculated only from the correctly received packets. Under the conditions with a reduced number of received packets, these values are presented descriptively and do not allow statistical inferences to be made about the general behavior of the link.

Validation of data storage and visualization

The data acquired by the sensors were transmitted to the buoy and subsequently stored in Firebase for visualization through

the web platform. Fig. 18 presents the time evolution of the pH (Fig.18-a) and turbidity (Fig. 18-b) values recorded during the tests. These graphs are used to verify the continuity of the information flow between the sensor node, the buoy, the database and the user interface.



Fig. 18. *Graph of pH sensor data over time (a) and graph of turbidity sensor data over time (b).*
Source: own elaboration.

The web platform allowed verifying the reception, storage and visualization of the data sent by the system. Fig. 19 shows, by means of cards, the RSSI, SNR, packet number, delay, payload size, battery level and timestamp of the last update. This validation confirms the functional integration between the sensor node, the buoy, Firebase and the web interface.



Fig. 19. *Real-time data obtained from the web platform through Firebase.*
Source: own elaboration.

Table 6: Comparison of tests performed in this and other related works

	Proposed system	**Tests at 433 MHz [5]**	**Tests at 2.4 GHz [3]**	**Tests at 2.4 GHz [4]**
Test environment	Swimming pool and 2 types of lagoon	Swimming pool	Swimming pool	Fish tank
Technology used	LoRa	TWS-433	Wi-Fi	Wi-Fi and Bluetooth
Measurement method	UW2OW (Submerged Node and Surface Node)	OW2OW (Both nodes at the surface)	UW2UW (Both nodes submerged)	UW2OW (Submerged node in fish tank and Surface Node)
Depth evaluated	0.25, 0.5 and 0.8 m	Surface	15 cm	Surface (15 cm)
Maximum distance with detectable reception	11.4 m (Swimming pool) 13 m (L. San Pablo) 8.5 m (L. Yahuarcocha)	9 m	16 cm	19 cm (Wi-Fi) 18 cm (Bluetooth)
Observed empirical RSSI threshold	−116 dBm	−116 dBm	Not present	−89 dBm
Other factors evaluated	SNR, Delay, Packet loss and web platform integration	Attenuation Free Space	RTT Packets received	Saltwater conditions

Source: own elaboration

DISCUSSION

The validation performed made it possible to verify the functional integration of the sensor node, the LoRa–Wi-Fi buoy, Firebase and the web platform in the three scenarios evaluated. The system received and displayed environmental information from a submerged node; however, the range and continuity of reception varied with depth and scenario. Therefore, the results should be interpreted as an operational validation of the prototype and not as a generalizable model of the underwater channel.

The approximate distance of 12.5 m obtained using MATLAB was similar in order of magnitude to some of the maximum distances recorded experimentally. Nevertheless, this proximity does not constitute an exact validation of the model. The simulation uses simplified conditions and reference parameters, whereas the measurements incorporate additional losses due to the enclosure, antennas, orientation, the water–air interface and environmental variability. Consequently, the model is used

only to contrast the general attenuation trend.

The difference between the nominal sensitivity of −137 dBm and the value close to −116 dBm observed before the practical loss of the link arises because both quantities represent different conditions. The first value corresponds to the nominal sensitivity of the transceiver for SF12 and a BW of 125 kHz under controlled conditions. The second represents an empirical threshold of the complete prototype in the scenarios evaluated. The losses introduced by the enclosure, the antenna, impedance matching, orientation, contact with water and the water–air interface reduce the available margin. For this reason, −116 dBm is not proposed as a universal LoRa threshold, but as a value observed for the implementation developed.

SNR values below or close to −20 dB should be interpreted as marginal reception conditions. The robustness of the modulation and error correction may allow occasional packet reception under these conditions, but the high loss percentages show that the link does not remain stable. Consequently, the reception of one or several packets at the limit is not sufficient to consider a given distance reliable.

The mean delays, ranging approximately between 5 and 6.4 s, correspond to the interval measured between the transmission of the packet at the sensor node and its reception at the communication buoy. These values are mainly related to the LoRa configuration selected to increase link robustness. The use of SF12 increases the duration of each symbol and, consequently, the airtime of the packet. Additionally, the Coding Rate 4/8, the 125 kHz bandwidth, the 12-symbol preamble, the payload size and the processing performed by the devices contribute to the total delay. These times may be acceptable for the periodic monitoring of slow-changing environmental variables, such as pH and turbidity, but they limit the use of the system in real-time control applications.

Losses above 60 % recorded near the maximum distances show the need to distinguish between distance with detectable reception and operating distance. The maximum distances represent the limit at which information was still received, whereas the operating distances constitute more conservative conditions for deployment. For future applications, local storage, retransmissions, reception confirmation and temporal redundancy could be incorporated; however, these mechanisms were not evaluated in the present study.

Related works show that the range of underwater electromagnetic communications depends on the frequency, the link configuration, the depth and the test medium (see Table 6). The proposal presented differs mainly by integrating a sensor node, a LoRa–Wi-Fi communication buoy, cloud storage and a web platform within a functional architecture. Distance comparisons should be interpreted with caution, because the studies use different antennas, frequencies, geometries and water conditions.

The limitations of the study include the use of a single LoRa configuration during the reported validation, the absence of a complete electromagnetic characterization of the antennas inside the enclosure, the use of reference physicochemical parameters in the simulation and the uncontrolled variability of the natural scenarios. Consequently, the results are valid for the prototype and the conditions evaluated, but should not be extrapolated directly to other water bodies.

CONCLUSIONS

The work made it possible to design, implement and functionally validate a short-range underwater monitoring architecture composed of a submerged sensor node, a LoRa–Wi-Fi communication buoy, a cloud database and a web platform. The prototype acquired, transmitted, stored and displayed environmental information in controlled and natural freshwater scenarios.

The validation showed that the depth and the conditions of each scenario affect the distance with detectable reception and the continuity of the link. The maximum distances do not necessarily represent reliable operation, due to the high loss percentages recorded near the limit. Therefore, deployment should use conservative operating distances and take into account that the effective threshold of the system may differ from the nominal sensitivity of the transceiver.

The configuration used generates delays of several seconds, so the architecture is appropriate for periodic monitoring of low-dynamics environmental variables, but not for real-time control. Future work includes optimizing the enclosure and the antennas, incorporating local storage and retransmission mechanisms, and evaluating communication strategies to extend coverage. These alternatives should be validated experimentally before their feasibility is asserted.

REFERENCES

[1] S. Ruiz and M. Muñoz, “Análisis de propagación de las comunicaciones ópticas subacuáticas.,” Escuela Superior Politécnica de Chimborazo, Jul. 2022, doi: 10.47187/perspectivas.5.2.200.

[2] F. Cuzme Rodríguez, A. Velasco Suárez, M. Domínguez Limaico, L. Suárez Zambrano, H. Farinango Endara, and M. Mediavilla Valverde, “Application for the Study of Underwater Wireless Sensor Networks: Case Study,” *Lecture Notes in Networks and Systems*, vol. 619 LNNS, pp. 124–136, 2023, doi: 10.1007/978-3-031-25942-5_11.

[3] C. S. Sendra, “‘Comunicaciones inalámbricas subacuáticas a 2,4 GHz para la transmisión de datos con altas tasas de transferencia’

TRABAJO FINAL DE GRADO," Universidad Politecnica de Valencia, Jan. 2011, Accessed: Aug. 04, 2024. [Online]. Available: https://riunet.upv.es/handle/10251/14605

[4] R. A. Arias, "Caracterización de sistemas de comunicación RF y ópticos en aplicaciones submarinas," Universidad Politécnica de Catalunya BarcelonaTech, Jul. 2022, Accessed: Aug. 04, 2024. [Online]. Available: https://upcommons.upc.edu/handle/2117/372768

[5] M. Delgado, S. Chango, and Benavidez. Mateo, "Uso de la banda de 433MHz para comunicaciones subacuáticas en ambientes controlados," *Universidad de las Fuerzas Armadas (ESPE)*, vol. 14, no. 2, pp. 1–6, Mar. 2024, doi: 10.24133/MASKAY.V14I2.3176.

[6] D. A. Jiménez Ballart, "Estudio de la cobertura de la modulación LoRa en la banda de 915[Mhz] en un ambiente urbano," Universidad de Chile, Santiago de Chile, 2018. Accessed: Mar. 10, 2025. [Online]. Available: https://repositorio.uchile.cl/handle/2250/168163

[7] H. M. Calero, "Red sensores multiservicio LPWAN LoRa, LoRaWAN, TTN y MQTT," Universitat Oberta de Catalunya, Jan. 2023, Accessed: Aug. 04, 2024. [Online]. Available: https://openaccess.uoc.edu/bitstream/10609/147334/6/caleroherruzo20TFM0123memoria.pdf

[8] F. Cuzme-Rodríguez, P. Otero, M. Á. Luque-Nieto, M. Domínguez-Limaico, and H. Farinango-Endara, "Underwater Wireless Sensor Networks and Cryptographic Applications," *Communications in Computer and Information Science*, vol. 1648 CCIS, pp. 46–58, 2022, doi: 10.1007/978-3-031-18272-3_4.

[9] K. Lin, T. Hao, W. Zheng, and W. He, "Analysis of lora link quality for underwater wireless sensor networks: A semi-empirical study," Asia-Pacific Microwave Conference Proceedings, APMC, vol. 2019-December, pp. 120–122, Dec. 2019, doi: 10.1109/APMC46564.2019.9038666.

[10] A. Dala and T. Arslan, "Design, Implementation, and Measurement Procedure of Underwater and Water Surface Antenna for LoRa Communication," *Sensors 2021*, Vol. 21, Page 1337, vol. 21, no. 4, p. 1337, Feb. 2021, doi: 10.3390/S21041337.

[11] A. Pozzebon, I. Cappelli, F. Campagnaro, R. Francescon, and M. Zorzi, "LoRaWAN Transmissions in Salt Water for Superficial Marine Sensor Networking: Laboratory and Field Tests," *Sensors*, vol. 23, no. 10, Art. no. 4726, 2023, doi: 10.3390/s23104726.

[12] Heltec, "HTIT-WB32LA_V3 LoRa Node Development Kit," *Heltec Automation*, vol. 1.1, Sep. 2022, Accessed: Apr. 12, 2024. [Online]. Available: https://heltec.org

[13] Firebase, "Firebase Realtime Database," Firebase. Accessed: Apr. 06, 2025. [Online]. Available: https://firebase.google.com/docs/database?hl=es-419

[14] M. Serrano, "¿Qué es la protección IP65? ¿En qué se diferencia con IP67? - IkolCrane," IkoCrane. Accessed: May 19, 2025. [Online]. Available: https://www.ikolcrane.com/aprender/que-es-la-proteccion-ip65

[15] S. J. Carrasquero, J. C. Marín, C. Muñoz, R. Vargas, C. Vargas, and P. Tuviñez, "Parámetros químicos medidos en las aguas de piscinas de los dos... | Download Scientific Diagram," *ResearchGate*, vol. 56, Jan. 2016, Accessed: Mar. 22, 2025. [Online]. Available: https://www.researchgate.net/figure/Parametros-quimicos-medidos-en-las-aguas-de-piscinas-de-los-dos-complejos-recreacionales_fig1_325654330

[16] J. Pabón, "Distribución y evaluación de la vegetación macrofítica en el lago de Yahuarcocha, Provincia de Imbabura," Universidad Técnica del Norte, Recursos Naturales Renovables, Dec. 2015, Accessed: Mar. 01, 2025. [Online]. Available: https://repositorio.utn.edu.ec/handle/123456789/6943

[17] S. O. Nelson, "Dielectric Properties of Agricultural Products: Measurements and Applications," *IEEE Transactions on Electrical Insulation*, vol. 26, no. 5, pp. 845–869, 1991, doi: 10.1109/14.99097.

[18] F. T. Ulaby and U. Ravaioli, FUNDAMENTALS OF APPLIED ELECTROMAGNETICS Eighth Edition. Pearson Education, 2023. Accessed: Mar. 22, 2025. [Online]. Available: www.pearsoned.com/permissions/.

[19] E. Navarro, "Desarrollo de un simulador de radar de apertura sintética y propuesta de diseño de radio frecuencia.," Esuela Técnica Superior de Ingeniería y Sistemas de Telecomunicaciones, 2017. Accessed: Mar. 23, 2025. [Online]. Available: https://oa.upm.es/52922/1/TFG_EDUARDO_NAVARRO_SABARIEGOS.pdf

[20] Semtech, "SX1261/2 Long Range, Low Power, Sub-GHz RF Transceiver," Datasheet. Accessed: Apr. 12, 2024. [Online]. Available: https://semtech.my.salesforce.com/sfc/p/#E0000000JelG/a/2R000000Un7F/yT.fKdAr9ZAo3cJLc4F2cBdUsMftpT2vsOICP7NmvMo

[21] A. Jaszczyszyn, A. G. Jaszczyszyn, M. Guiguet, and H. D. Ramón, "Comparación de una red LoRaWAN con modelos de propagación en un entorno con vegetación de soja," *Elektron*, vol. 8, no. 2, pp. 101–106, Dec. 2024, doi: 10.37537/rev.elektron.8.2.203.2024.

ACKNOWLEDGMENTS

The authors thank Universidad CESMAG, Colombia, where the initial advances of this work were presented during the 3rd SAFARIS TECH INTERNATIONAL 2025 Congress. This manuscript extends that version through the complete implementation of the architecture, validation in aquatic scenarios and discussion of its operational limitations. They also thank the Renewable Natural Resources program of Universidad Técnica del Norte, Ecuador, for providing the laboratory spaces for sensor calibration; Fernando Guerra Goyes, for providing the Ubiquiti Loco M2 antenna; and Franco Elías Montezuma and Grace Gisel Cuasqui, for their collaboration during the experimental tests. MATLAB R2025a was used to implement the reference simulation model.

FUNDING

The authors declare that this research work received no public or private funding of any kind, nor is it part of any project with economic support.

CONFLICT OF INTEREST

None

AUTHORSHIP CONTRIBUTIONS

Conceptualization: Jaime Michilena-Calderón and Fabián Cuzme-Rodríguez;

Methodology: Jaime Michilena-Calderón and Fabián Cuzme-Rodríguez;

Software: Diego. Montezuma-Rosero;

Validation: Fabián Cuzme-Rodríguez, Jaime Michilena-Calderón and Luis Suárez-Zambrano; Formal analysis: Diego Montezuma-Rosero and Fabián Cuzme-Rodríguez;

Investigation: Diego Montezuma-Rosero; resources: Jaime Michilena-Calderón and Luis Suárez-Zambrano;

Data curation: Fabián Cuzme-Rodríguez;

Writing—original draft: Diego A. Montezuma-Rosero;

Writing—review and editing: Fabián Cuzme-Rodríguez, Jaime Michilena-Calderón and Luis Suárez-Zambrano;

Visualization: Diego Montezuma-Rosero;

Supervision: Jaime Michilena-Calderón;

Project administration: Jaime Michilena-Calderón;

SUPPLEMENTARY MATERIAL

Disponibilidad de materiales y datos: datos disponibles en GitHub, https://github.com/ArbeyCr/LoRa_Subacuatico